

AperTO - Archivio Istituzionale Open Access dell'Università di Torino

## New insights into UTSA-16

### **This is the author's manuscript**

*Original Citation:*

*Availability:*

This version is available <http://hdl.handle.net/2318/1601096> since 2022-01-28T16:34:33Z

*Published version:*

DOI:10.1039/c5cp05905d

*Terms of use:*

Open Access

Anyone can freely access the full text of works made available as "Open Access". Works made available under a Creative Commons license can be used according to the terms and conditions of said license. Use of all other works requires consent of the right holder (author or publisher) if not exempted from copyright protection by the applicable law.

(Article begins on next page)

## New insight in UTSA-16

---

Alessio Masala<sup>a</sup>, Jenny G. Vitillo<sup>a</sup>, Francesca Bonino<sup>a</sup>, Maela Manzoli<sup>a</sup>,  
Carlos A. Grande<sup>b</sup> and Silvia Bordiga<sup>\*a</sup>

<sup>a</sup>Chemistry Department, NIS and INSTM reference Centres, University of Torino, Via Quarello 15/A, 10135 Torino, Italy. <sup>b</sup>SINTEF Materials and Chemistry, P.O. Box 124 Blindern, N0314 Oslo, Norway

### List of contents

- Powder X-RD Figure S1
- Elemental analysis by means of energy dispersive X-ray spectroscopy (EDX).Table S1
- DRS-UV-Vis NIR of UTSA-16 Figure S2
- CO<sub>2</sub> uptake Table S2
- Specific heat capacity Figure S3
- MID-IR of CO and CO<sub>2</sub> adsorbed on UTSA-16 Figure S3
- Dual-site Langmuir model fit parameters for CO<sub>2</sub> adsorption isotherms Table S3
- Zero-coverage heat of CO<sub>2</sub> adsorption Table S4
- References

## Supporting tables and figures

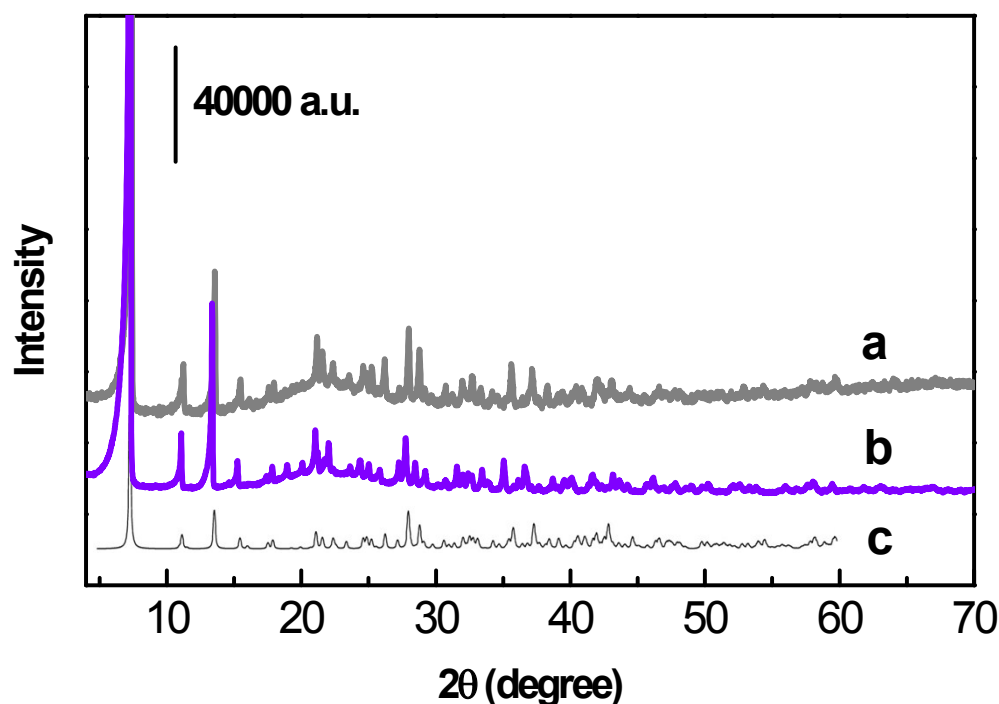


Fig. S1 Powder X-ray diffraction patterns of UTSA-16. Experimental powder diffraction pattern of **a**) as-synthesized UTSA-16 sample (grey line) and **b**) after activation over night at 363 K. (violet line). **c**) Simulated powder diffraction pattern obtained from the structure reported in Ref.<sup>1</sup>.

Tab. S1 UTSA-16 elemental analysis by means of energy dispersive X-ray spectroscopy (EDX).

Analysis parameters:

Magnification: 30000 X  
Accelerating voltage (kV): 300.00  
Tilt (deg): 0.0  
Elevation (deg): 17.8  
Azimuth (deg): 0.0

Specimen	K ato.%	Co ato.%	K:Co ato. ratio
1	5.51	7.61	1.38
2	5.44	7.5	1.38
3	4.04	5.19	1.28
4	6.6	8.78	1.33
5	6.28	8.68	1.38

6	5.41	7.24	1.34
7	3.83	5.3	1.38
8	4.05	5.52	1.36
9	3.82	5.09	1.33
10	4.71	6.37	1.35
11	4.92	5.74	1.17
12	4.22	5.58	1.32
13	4.38	6.05	1.38
14	3.24	4.3	1.33
15	5.53	7.1	1.28
16	3.23	4.23	1.31
17	4.35	5.8	1.33
18	4.09	5.55	1.36
19	5.37	7.28	1.36
20	4.49	5.86	1.31
21	5.85	8.8	1.5

The average value of K:Co found in 21 UTSA-16 particles is **1:1.34**.

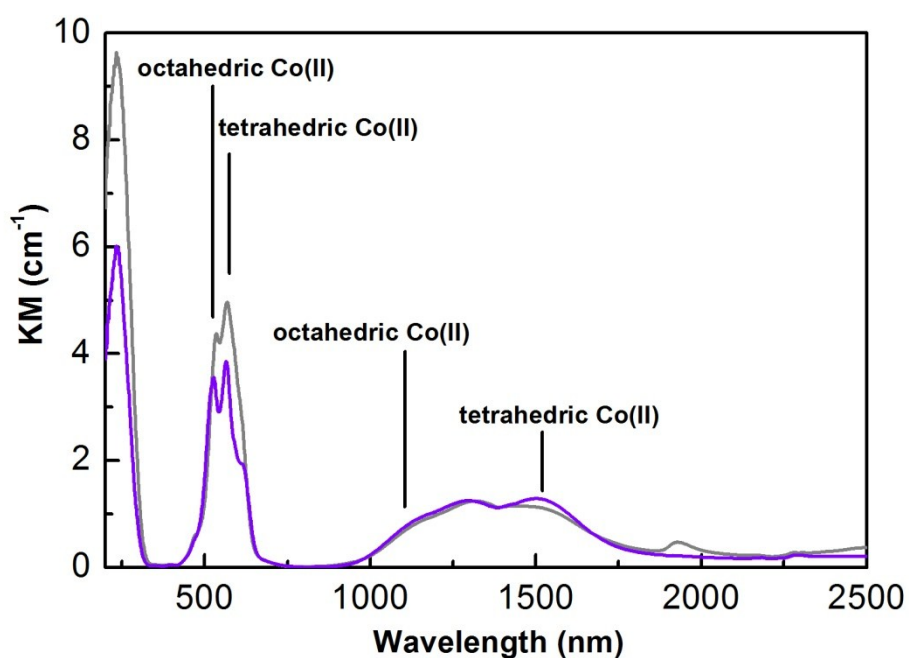


Fig. S2 DR-UV-VIS spectra of as-synthesized and activated UTSA-16 (grey and violet lines respectively).

Tab. S2 Review of CO<sub>2</sub> uptakes by some relevant MOFs at the typical CO<sub>2</sub> partial pressure in post-combustion CCS.

Adsorbent	CO <sub>2</sub> uptake at 0.15 bar (wt %)	Temperature (K)	Reference
Ni-CPO-27	16.9	298	2,3
HKUST-1	11.6	293	4
UTSA-16	11.1	298	Present work
mmen-Cu-BTTri	9.5	298	5
MIL-47	1.1	298	3
ZIF-100	1.0	298	6
IRMOF-3	0.6	298	3,7

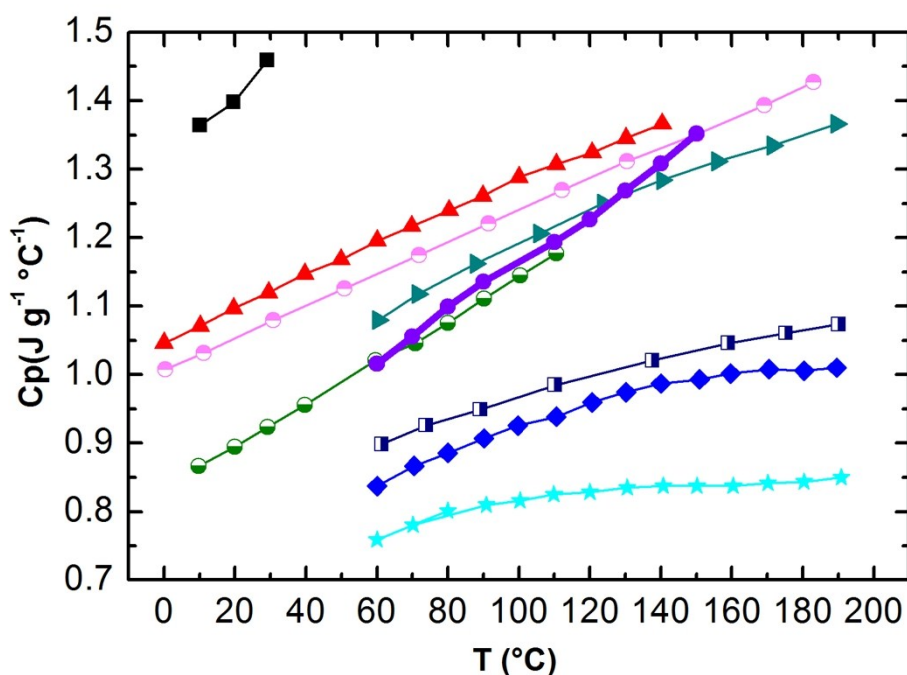


Fig. S3 Comparison of specific heat capacity of UTSA-16 with other MOFs. From top to bottom, Mg-BTC (■ black)<sup>8</sup>, Co-BTC (▲ red)<sup>9</sup>, DWCNT (● magenta)<sup>10</sup>, Ni-BTB (▶ dark cyan)<sup>11</sup>, UTSA-16 (● violet, bold line), Mn-BDC (● olive)<sup>9</sup>, LaBTB (□ navy)<sup>11</sup>, MOF-177 (◆ blue)<sup>11</sup>, IRMOF-1 (★ cyan)<sup>11</sup>. It is evident as UTSA-16 shows suitable Cp for CCS applications.

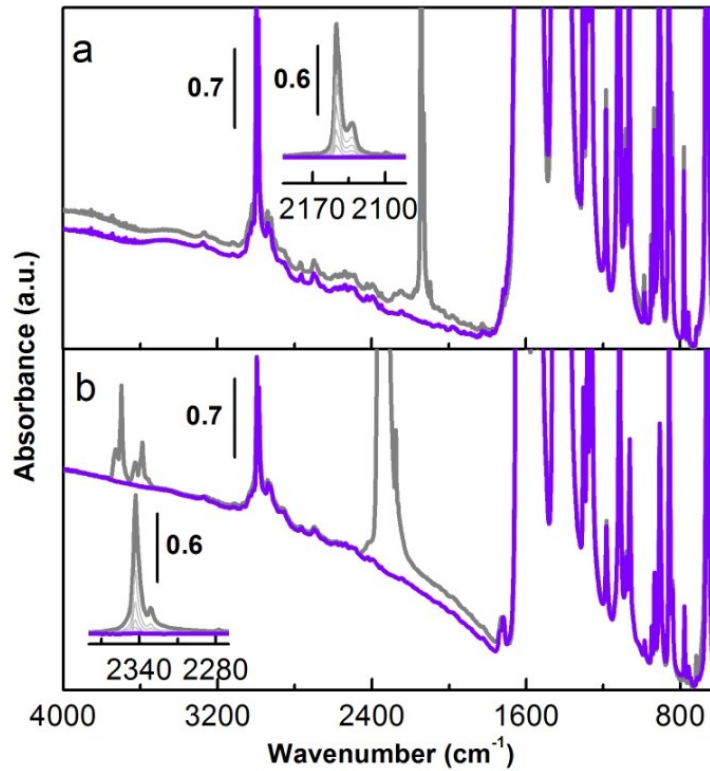


Fig. S4. FTIR spectra of activated UTSA-16 probed by CO and CO<sub>2</sub>. a) Spectrum recorded in presence of 20 mbar of carbon monoxide (grey line). The inset shows the effect of progressive outgassing in the  $\nu(\text{CO})$  region. b) Effect of 10 mbar of CO<sub>2</sub> (grey line). The inset reports the effect of progressive outgassing in the  $\nu_3(\text{CO}_2)$  region. Spectra reported in the insets are background subtracted. In both (a) and (b) parts, the IR spectrum of activated UTSA-16 is reported (violet line).

Tab. S3 Dual-site Langmuir model fit parameters for CO<sub>2</sub> adsorption isotherms of UTSA-16 at 273, 298 and 313 K and 1 bar

<p><b>T = 273 K:</b></p> $q \equiv q_A + q_B = \frac{q_{sat,A} b_A p}{1 + b_A p} + \frac{q_{sat,B} b_B p}{1 + b_B p}$ $q_{sat,A} = 5.005 \text{ mmol g}^{-1}$ $q_{sat,B} = 0.05 \text{ mmol g}^{-1}$ $b_A = 2.094554 * 10^{-4} \text{ Pa}^{-1}$ $b_B = 3.5 * 10^{-4} \text{ Pa}^{-1}$
<p><b>T = 298 K:</b></p> $q \equiv q_A + q_B = \frac{q_{sat,A} b_A p}{1 + b_A p} + \frac{q_{sat,B} b_B p}{1 + b_B p}$ $q_{sat,A} = 5.015 \text{ mmol g}^{-1}$

$$q_{sat,B} = 0.5 \text{ mmol g}^{-1}$$

$$b_A = 6.29836 * 10^{-5} \text{ Pa}^{-1}$$

$$b_B = 1.81628 * 10^{-7} \text{ Pa}^{-1}$$

**T = 313 K:**

$$q \equiv q_A + q_B = \frac{q_{sat,A} b_A p}{1 + b_A p} + \frac{q_{sat,B} b_B p}{1 + b_B p}$$

$$q_{sat,A} = 5.401714 \text{ mmol g}^{-1}$$

$$q_{sat,B} = 0.05424 \text{ mmol g}^{-1}$$

$$b_A = 2.28 * 10^{-5} \text{ Pa}^{-1}$$

$$b_B = 2.19 * 10^{-5} \text{ Pa}^{-1}$$

Variables index:

$q_{A(B)}$  = adsorbed quantity of CO<sub>2</sub> by site A (B) at pressure p.

$q_{sat,A(B)}$  = maximum adsorbed quantity of CO<sub>2</sub> by site A (B) at saturation pressure.

$b_{A(B)}$  = Langmuir constant for the site A (B).

Tab. S4 Zero-coverage heat of CO<sub>2</sub> adsorption on some selected MOFs. All Q<sub>st</sub> values were originally determined by a fitting to the published adsorption isotherms.

Adsorbent	-Q <sub>st</sub> (kJ/mol)	Technique	Reference
Ni-CPO-27	42	Clausius-Clapeyron	12
UTSA-16	39.7	Clausius-Clapeyron	Present work
HKUST-1	35	Clausius-Clapeyron	13
IRMOF-1	34	Clausius-Clapeyron	14

## Reference

- Xiang, S., Wu, X., Zhang, J., Fu, R., Hu, S and Zhang, X., *J. Am. Chem. Soc.*, 2005, **127**, 16352–16353.
- P. D. C. Dietzel, V. Besikiotis and R. Blom, *J. Mater. Chem.*, 2009, **19**, 7362–7370.
- A. Ö. Yazaydin, R. Q. Snurr, T.-H. Park, K. Koh, J. Liu, M. D. LeVan, A. I. Benin, P. Jakubczak, M. Lanuza, D. B. Galloway, J. J. Low and R. R. Willis, *J. Am. Chem. Soc.*, 2009, **131**, 18198–18199.
- P. Aprea, D. Caputo, N. Gargiulo, F. Iucolano and F. Pepe, *J. Chem. Eng. Data*, 2010, **55**, 3655–3661.
- T. M. McDonald, D. D'Alessandro, R. Krishna and J. R. Long, *Chem. Sci.*, 2011, **2**, 2022–2028.

- 6 B. Wang, A. P. Côté, H. Furukawa, M. O'Keeffe and O. M. Yaghi, *Nature*, 2008, **453**, 207–211.
- 7 A. R. Millward and O. M. Yaghi, *J. Am. Chem. Soc.*, 2005, **127**, 17998–17999.
- 8 L.-F. Song, C.-H. Jiang, J. Zhang, L.-X. Sun, F. Xu, Y.-Q. Tian, W.-S. You, Z. Cao, L. Zhang and D.-W. Yang, *J. Therm. Anal. Calorim.*, 2009, **101**, 365–370.
- 9 C.-H. Jiang, L.-F. Song, J. Zhang, L.-X. Sun, F. Xu, F. Li, Q.-Z. Jiao, Z.-G. Sun, Y.-H. Xing, Y. Du, J.-L. Zeng and Z. Cao, *J. Therm. Anal. Calorim.*, 2010, **102**, 1087–1093.
- 10 G. G. Silva, A. W. Musumeci, A. P. Gomes, J.-W. Liu, E. R. Waclawik, G. A. George, R. L. Frost and M. A. Pimenta, *J. Mater. Sci.*, 2009, **44**, 3498–3503.
- 11 B. Mu and K. S. Walton, *J. Phys. Chem. C*, 2011, **115**, 22748–22754.
- 12 P. D. C. Dietzel, R. E. Johnsen, H. Fjellvåg, S. Bordiga, E. Groppo, S. Chavan and R. Blom, *Chem. Commun.*, 2008, 5125–5127.
- 13 D. S. Qing Min Wang, *Microporous Mesoporous Mater.*, 2002, 217–230.
- 14 Z. Zhao, Z. Li and Y. S. Lin, *Ind. Eng. Chem. Res.*, 2009, **48**, 10015–10020.